Evaluating the Accuracy of Modified Near-Infrared Camera with Wide FOV in Monitoring Crop Health

Ghimire, S.,[1] and Horanont, T.[2]
School of Information, Computer and Communication Technology (ICT), Sirindhorn International Institute of Technology, Thammasat University, 131 Moo 5, Tiwanont Road, Bangkadi Muang Pathum Thani 12000 Thailand, E-mail: ghimire.aiesecer@gmail.com[1], teerayut@siit.tu.ac.th[2]

Abstract
Unmanned aerial vehicle (UAV) equipped with multispectral sensors have become an active research topic for crop health monitoring, across many regions. However, the high cost associated with such sensors suggests us to shift to a cheaper alternative in order to be implemented by average farmers from developing countries. In this study, we evaluated the potential of a lightweight (38 gm) mobius action camera with wide field of view (FOV) in monitoring crop health through the removal of IR filter, and replacing it with Wratten 25A red filter. The research implemented Structure from motion (SfM) for creating orthomosaic, which was followed by the computation of Normalized Difference Vegetation Index (NDVI). Finally, the results of NDVI from the modified camera was linearly correlated with the field measurements of Leaf Area Index (LAI), carried using LI-COR LAI 2000 Plant Canopy Analyzer, having the coefficient of determination (R^2) of 0.843. The results obtained from the validation demonstrate that the modified camera setup has good potential for monitoring crop health.

1. Introduction

Remote sensing technologies have been providing timely and accurate information related to crop health and productivity; and have been widely used in agricultural health monitoring at both regional and global scale since decades (Atzberger, 2013). One of the important characteristics for any agricultural health monitoring system is to timely disseminate information related to plant health, growth, and yield to the farmers. With recent technological advancements, a lightweight airborne remote sensing (Zhang and Kovacs, 2012) presents a unique advantage over traditional satellite borne images (Lamb and Brown 2001), in terms of high spatial and temporal resolution with reduced effect of cloud cover during data acquisition. However, the associated cost with multispectral sensors are generally high, which suggests researchers to focus on a cheaper alternative that could be financially implemented by farmers from developing countries.

Not surprisingly, there have been several studies in the application of sensor networks, information processing and decision support for precision agriculture (Allahyari et al., 2016, Shaw et al., 2016 and Alexandridis et al., 2017). Likewise, the remote sensing platforms including air and space borne suffers atmospheric scattering in the blue and green regions, consequently it is recommended to use longer wavelengths such as red and near-infrared (NIR) for agricultural applications (Nijland et al., 2014). Therefore, an inexpensive digital camera setup, with internal infrared filter removed and replaced with blue blocking filter allowed blue channel to record the NIR light, while red recorded in its original channel (Zigadlo et al., 2001 and Hunt et al., 2010), demonstrated a promising technique for agricultural health monitoring. In recent years, a lot of research have implemented such modification of standard RGB digital camera to near infrared for the assessment of crop health (Hunt et al., 2010, Rabatel et al., 2014 and Hunt et al., 2005), but very less has been explored in complementary metal-oxide semiconductors (CMOS) based action camera model (Wijitdechakul et al., 2016a and Ghazal et al., 2015). For instance, (Hunt et al., 2010) studied the ability of charge-coupled device (CCD) based digital sensors in crop monitoring by embedding in UAV platform. Their results in terms of green normalized vegetation index (GNDVI) was found to have a good correlation with leaf area index (LAI) suggesting that their approach was potential in providing accurate information related to crop health. Similarly, (Wijitdechakul et al., 2016a) demonstrated a dual action camera model: one normal RGB camera while the other IR filter removed modified camera in UAV platform for real-time agricultural area management. Their system was able to detect the healthy vs non-healthy plantations, and notify farmers regarding their unhealthy plantation area for improved decision making in agricultural practices.

The action cameras offers a unique advantage in UAV photogrammetry due to its lightweight and low-cost (Hastedt et al., 2016). A significant amount of research has been performed on evaluating the application of action cameras for UAV photogrammetry (Hastedt et al., 2016, Balletti et al., 2014 and D'Agostino et al., 2015). For instance, (Hastedt et al., 2016) highlighted different camera calibration approach on the GoPro Hero4 model to evaluate the potential of a pre-correction step in rectifying the initial distortion introduced by the wide angle lens for the application in UAV photogrammetry. They also discussed about the challenges introduced by such lenses, in terms of its short principal distance and high radiometric distortion, which causes deviation from the central projective model.

An efficient method for image matching was applied by (Agarwal et al., 2011), where they identified a small number of candidates for each image using vocabulary tree recognition instead of matching all the image together, which still preserved the features for SfM, and significantly reduced the processing time. Similarly, the linear time SfM was implemented for large scale image reconstruction (Wu, 2013) by introducing a preemptive feature matching process, which reduced the image matching process by 95%, while still recovering sufficient good feature matches for the reconstruction process. Likewise, (Turner et al., 2012) presented an automated technique for image mosaicking by implementing UAV photogrammetry and SfM algorithm. The images were processed to create the three dimensional point clouds in an arbitrary coordinate space, which was later transformed into global coordinate system using; a. direct camera EXIF file, b. ground control points. Thus, the point clouds were used to generate a digital terrain model, which was followed by the creation of an orthomosaic. Their results demonstrated an absolute spatial accuracy of 65-120 cm with direct georeferencing method, and 10-15 cm using ground control points (GCP) technique.

All the above literatures were very significant in adapting the methodological workflow for this study. The purpose of this research was to assess the potential of an inexpensive modified CMOS based action camera model with blue blocking filter to monitor crop health in banana plantations using vegetation indices specifically, NDVI. This study also applied different camera calibration approach for; a. removal of distortion introduced by fish eye lens, and b. calibrating spectral signatures, to assess the potential of modified camera system in UAV photogrammetry.

2. Research Needs and Design

Banana plantation plays a great role in food security and income generation for millions of the region's rural poor in Thailand. It is also a popular staple food which is rich in vitamins and minerals, and contributes approximately US $2.3 million each year in the economy (Anupunt, 2002). However, the plantation is affected by several biotic and abiotic stress factors. Biotic stress includes fungi, bacteria, viruses, weeds and pests, while the abiotic stress includes influence of the surrounding environment for example, water and temperature etc. Specifically, the disease "Black Sigatoka" (Mobambo et al., 1993) affects banana plantation and its yield by obstructing the photosynthetic process, blackening and reducing the leaf area. Therefore, predicting plantation response to crop stress is important in developing strategies, and enables decision-making for use by farmers and researchers to develop a better response mechanism and resilient agricultural systems.

The methodology adopted in this study enabled the spatial analysis within banana plantation, leading to potential application in the improvement of plantation health and agricultural management using the modified camera. Furthermore, monitoring of photosynthetic activity using NDVI, at an early stage will provide farmers with valuable spatial information regarding the crop health, and disease within their plantation that helps prevent yield loss. This methodological framework using an inexpensive modified infrared camera presented an alternative crop health monitoring system targeted for farmers in developing countries. The workflow for the research design has been presented in Figure 1.Firstly, the images were captured using the modified camera embedded in UAV, which were then preprocessed and calibrated before running SfM algorithm based on (LLC, 2017). The result of SfM algorithm outputs an orthomosaic, using which we computed NDVI.

3. Materials and Methods

3.1. Study Site and Data Acquisition

The study area consists of *Musa acuminata* plantation; a species native to Southeast Asian region; which covers an area of 0.186 sq.km as represented by the red polygons in Figure 2. The area's center is located at N 14° 15.133′ E 100° 53.393′ and Z 10 meters (WGS84) in Pathumthani province, Thailand. The area in yellow polygon covers 0.0445 sq.km, which has been indicated as the dedicated area for the comparison and validation of NDVI results, with the field estimates of LAI using LI-COR LAI 2000 Plant Canopy Analyzer.

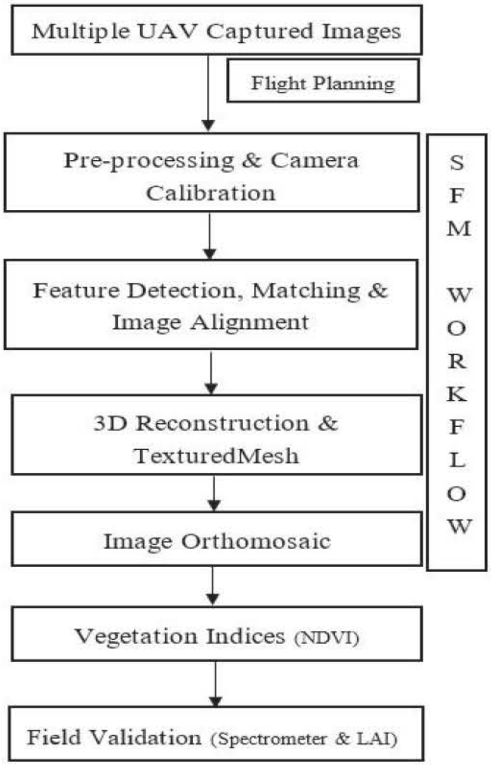

Figure 1: Workflow design for modified infrared CMOS sensor

3.2 Modified Camera System

The camera system used for the research was a lightweight (38 gm.) mobius action camera as demonstrated in Figure 3(a), having the dimension of (61 mm * 35 mm * 18 mm), and CMOS based camera sensor with a spectral response range of 400-1000 nm; similar to most of the CCD based camera model. The spectral sensitivity of the mobius action camera was measured in a completely dark room using Black Comet C-200 TEC Stellar Net Spectrometer as shown in Figure 3(b). After the removal of infrared blocking filter, the sensor was illuminated with an 850nm monochromatic led light, and the results demonstrate that the camera was more sensitive to near infrared spectrum in its blue channel and least in its red channel.

Since, the sensitivity of NIR was higher at blue channel, the camera was modified by replacing its IR filter with Wratten 25A red filter, which is a gelatin filter that restricts blue and green bands ranging(440- 600 nm) while allows red(550-850nm) and near infrared(800-1000 nm) (Velasquez et al., 2016). Thus, the camera sensor records Red-Green-NIR configuration, with NIR recorded in its blue channel. Typically, the use of action camera with wide angle lens (FOV 87mm) requires processing to correct fish eye effect for a better performance of SfM algorithm (Hastedt et al., 2016 and Balletti et al., 2015). The preprocessing step has been described in detail below.

3.2.1 Geometric calibration of wide angle lens

The imaging system, in most of the action camera with wide angle lens deviates from central projective model. Additionally, CMOS sensors in action camera doesn't follow global shutter camera models, which forms the basis for SfM approach (Hedborg et al., 2012). Therefore, it is desired to apply pre-correction in the image for producing it closer to central projective model (Hastedt, 2016). An initial preprocessing step was implemented by applying the lens distortion correction plugin in GIMP 2.8.16, to correct the initial correction introduced by wide angle lens. The correction for the remaining distortion was estimated using standard checkerboard pattern (7x9), which implemented the pre-calibration approach similar to (Harwin et al., 2015). For the correction of lens distortion, we implemented the distortion model (Duane, 1971, Kelcey and Lucieer, 2012 and Hastedt et al., 2016), which computed both the radial and tangential components of lens distortion. A set of 8 images of the checkerboard kept in fixed position was taken from various angles, and the images were loaded onto the Agisoft Lens. This software generates camera orientation parameters and lens distortion coefficients using the model (Duane, 1971); based on bundle adjustment of matched corners of the checkerboard pattern. The generated parameters were then exported to xml file format, which was later supplied to Agisoft Photoscan for calibrating the field images.

3.2.2 Radiometric Calibration

The goal of calibration was to convert the pixel value of each channel to reflectance. For the calibration of the images, we implemented the plugin (Horning, 2013), which works with Fiji image processing software (Schindelin et al., 2012). First, the plugin calculates the calibration parameters, followed by applying those generated parameters to a directory of images. For calibration, all the images must have same camera settings (shutter speed, ISO etc.) as the image which was used to calculate the calibration parameters.

Figure 2: The study area in Pathumthani province, Thailand. The red polygon represents the distribution of banana plantation, while the yellow polygon represents the area for the validation of NDVI

(a) (b)

Figure 3: (a) Modified infrared camera setup with 3 axis brushless gimbal on DJI P3 Professional, (b) Spectrometer (Black Comet C-200 TEC ranging from 200-1100nm)

The plugin allowed flexibility in subtracting a percentage of the NIR pixel values from the visible channel. This was because after modification, some percentage of NIR light gets mixed in all the visible channel. The value to subtract was determined by taking an image over 850 nm LED illumination and carefully studying the histogram of each channels. The plugin also supports the removal of gamma effect (Lebourgeois et al., 2008), that is normally applied when the image gets converted to a JPEG inside the camera making the camera sensor mimic the response of a human eye. The camera sensor records light intensity linearly, but our eyes are more sensitive to low-light conditions than they are to the brighter lighting, therefore, the gamma correction was applied. The linear regression was performed between average pixel value for red band and the reference reflectance recorded by standard reflectance target at 600 nm, and similar for NIR but at 850 nm.

Finally, the slope and aspect obtained from the linear regression was applied using gain offset method on each bands to produce the reflectance images.

3.3 Feature Detection, Matching and Alignment

Image matching is one of the most time consuming steps in SfM (Verhoeven, 2011). To reduce the processing time, the implemented SfM algorithm (Javernick et al., 2014 and LLC, 2017) firstly detected the pair of image which shared the same view, and generated the descriptors for each point; and finally detected its equivalence points across the images based on a similar approach to SIFT (Lowe, 2004) as mentioned in (Sona et al., 2014). Furthermore, the value of 50,000 and 5,000 were supplied as the number of key points and tie points to be extracted from each image, i.e. the algorithm (LLC, 2017) extracted 50,000 points out of which it selected 5000 best points from each image for the alignment process, which reduced the associated processing time. These descriptors and its correspondence across the images allowed the creation of 3D sparse point cloud reconstruction (Verhoeven et al., 2012) and camera positions (Hartley and Zisserman, 2004 and Ullman 1979) as shown in the Figure 4.

3.4 3D Reconstruction and Orthomosaic

This step applied the camera calibration parameters previously obtained from Agisoft Lens (LLC, 2017) using the distortion model (Duane, 1971) to remove the lens distortion before further processing the 3D reconstruction (Verhoeven, 2011). Given a set of aligned sparse point clouds and calibration coefficients, the algorithm applied classic bundle adjustment (Sona et al., 2014 and Bendig et al., 2015) to generate dense point cloud. The dense reconstruction utilized all pixel values (Scharstein and Szeliski, 2002), which allowed handling of the small details in the scene represented as a mesh (Verhoeven, 2011). Furthermore, the mesh were textured using the multiple images. Since, our modified camera model didn't have the GPS embedded within the system, therefore, the dense reconstructed textured mesh were still in an arbitrary coordinate system. To transform it to an absolute coordinate system, we collected 8 GCPs using a GPS, and after that the set of GCP were supplied and identified manually in the interface; the algorithm (LLC, 2017) computed seven parameters Helmert Transformation (Javernick et al., 2014 and Verhoeven et al., 2012). The parameters like scale factor, translation and rotation matrix were computed based on matched feature points and GCPs (Turner and Watson, 2012).

The final phase was to merge the images into a single mosaic covering whole study area. As all the images were georectified, it was a simple process to mosaic them using a mosaicking algorithm implemented in (LLC, 2017).

4. Results

4.1 Alignment Accuracy

An approach similar to (Balletti et al., 2014) has been implemented for the alignment of the 89 images using algorithm defined in (LLC, 2017). First of all, the images were corrected for the initial distortion using Agisoft Lens (LLC, 2017). Before applying the calibration parameters, a pre-correction step (Hastedt et al., 2016 and Balletti et al., 2014) was introduced to increase the accuracy, reliability, and provide valid parameters to correct the wide angle images into central projective mathematical model using GIMP 2.8 (Distortion, 2013). After the pre-correction step, the images were aligned using Agisoft Photoscan 1.2.4 (LLC, 2017) using generic image pair selection supplying the key point and tie point limit of 50,000 and 5,000 respectively. The medium accuracy was chosen for the alignment process which subsequently reduced the matching and alignment time to 49 seconds and 25 seconds respectively. The accuracy (RMSE error) of the alignment process improved significantly from 0.0975 m to 0.0365 m with the mean key point size and effective overlap of 6.89094 pixel and 2.7732 respectively, after the introduction of the precorrection step.

4.2 Spectral Calibration of the Modified Camera

The spectral calibration of the modified mobius camera was performed with 5 calibration targets using Black Comet C-200 TEC Stellar Net Spectrometer as shown in Figure 3(b). The calibration process was carried on July 7, 2017 simultaneous to the drone flight data acquisition, to maintain same atmospheric conditions. The spectrometer readings of % reflectance were linearly correlated with the normalized image pixel values (DN) collected using modified camera during same time of the day; in a plugin (Horning, 2015) where, the reflectance values were supplied using a csv file. The reference spectrum for visible (red) had a good correlation with image pixel values at 600 nm with R^2 value of 0.939, and near-infrared spectrum at 850 nm with R^2 value of 0.9059. Finally, the plugin (Horning, 2013) applied the calibration parameters of regression model to the directory of images for the calibration of modified infrared camera, which later supported the calculation and validation of NDVI results, described in the section below.

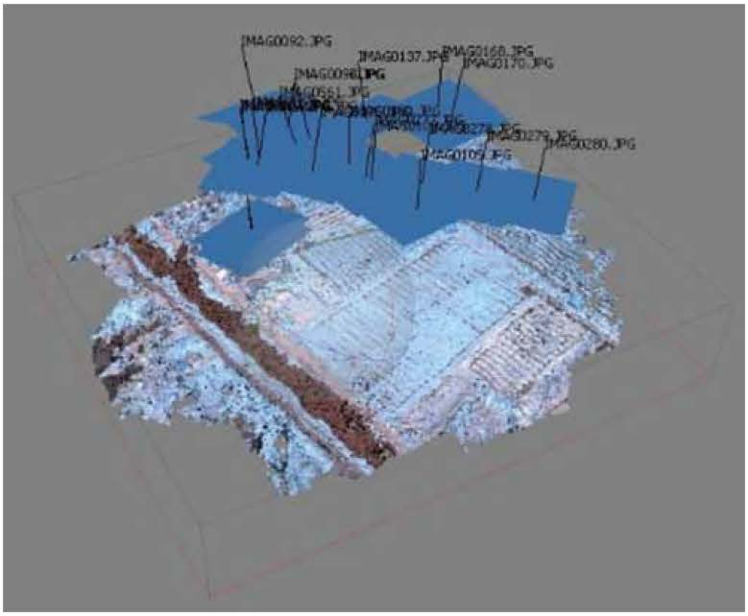

Figure 4: Image Alignment where, the blue polygons on the top represents each camera positions

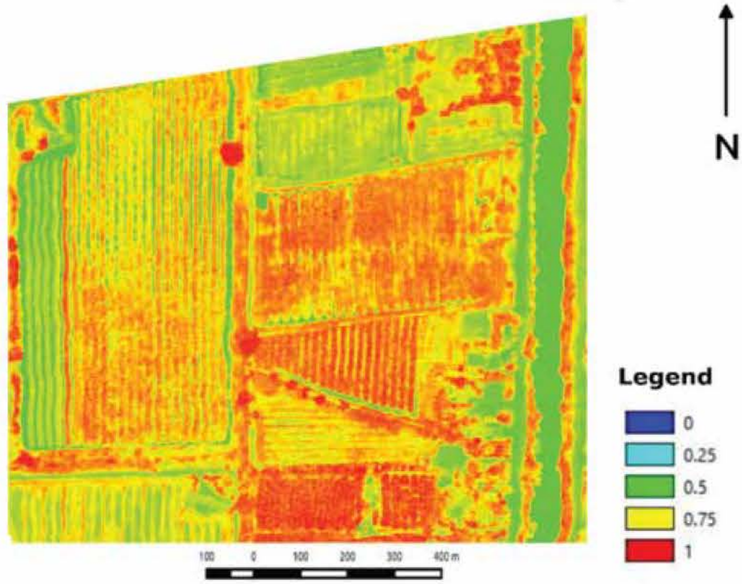

Figure 5: NDVI computation from modified infrared camera

4.3 Normalized Difference Vegetation Index

The Normalized Difference Vegetation Index (Tucker et al., 2001) is an indicator that applies the visible and near-infrared channel within the electromagnetic spectrum. NDVI has a wide application (Meng et al., 2013) in vegetative studies, as it has been widely used to estimate crop yields, access plant health, and estimate biophysical characteristics like LAI. As mentioned in many literatures (Fan et al., 2009b, Bravo et al., 2003 and Marti et al., 2007), NDVI has positive correlation with field estimates of leaf area index and the amount of biomass. These indices takes on values between -1 and 1; with -1 being no vegetation (rock, water, bare soil) and 1 being the healthy and highly photosynthetic vegetation. The result of NDVI has been demonstrated in Figure 5 and takes the form as Equation (1).

$$NDVI = (NIR-RED) / (NIR+RED)$$

Equation 1

(a)

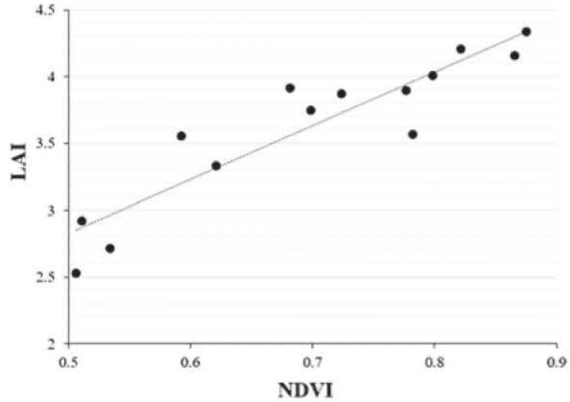

(b)

Figure 6: (a) Field validation using LI-COR LAI 2000 Plant Canopy Analyzer, (b) Scatterplot depicting the linear relationship between field estimate of LAI and NDVI

Finally, we designed 18 square plots, each measuring the length of 5m, distributed in an area of 0.0455 sq.km; for the validation of NDVI. The field measurements of LAI followed a nondestructive approach, using LI-COR LAI 2000 Plant Canopy Analyzer as shown in Figure 6(a). Simultaneous to the ground measurements, we recorded the aerial images with modified near-infrared camera at an altitude 60 m directly above the plot center in each individual plots. The linear relationship between NDVI and field measured LAI was investigated to validate the results from the modified infrared camera, which followed a similar approach to (Hunt et al., 2010). This was based on the literature (Fan et al., 2009a) which demonstrated NDVI as a good estimator of LAI. Some of the plots encountered saturation in NDVI values above the LAI of 4.5 (Turner et al., 2007), which was supported by the fact that most of the vegetation indices suffer saturation at some point of LAI which has been mentioned in (Gitelson et al., 1996 and Hunt et al. 2010). The four plots that suffered saturation were removed as suggested in (Hunt et al., 2010), which resulted in an improved correlation, with the coefficient of determination (R^2) of 0.843 as shown in Figure 6(b), where the relationship between the two variables were expressed linearly as: LAI = 4.0374 NDVI + 0.8066. Finally, these results indicate that the modified camera has a great potential in monitoring crop health.

5. Discussion

Many different approach have been applied for the correction of wide angle lens introduced by CMOS sensors. For instance, calibration of action camera specifically, GoProHero3 for photogrammetric purpose has been evaluated by (Balletti et al., 2014), with the recommendation of use of high spatial resolution during data acquisition. They applied checkerboard pattern and OpenCV algorithms to generate distortion free images, which significantly improved the accuracy in image registration. The alignment accuracy of the initial distorted images were 0.035 m, which later halved to 0.015 m using the undistorted images. An algorithm for robust and automatic camera calibration using chessboard pattern has been presented by (Douterloigne et al., 2009). They discussed on the variation of the camera parameters, especially on the second order un-distortion parameters, which was explained by different random camera positions, giving more weight to one area of the image than another. As a result, they suggested to apply as much views as possible for the correction and generation of accurate results. One must also pay great attention towards image capture of the checkerboard pattern to get rid of the bad lighting, low luminance and gloss effect while imaging from different viewing angles, as this might create confusion and block the algorithm from creating good matches between the images (Balletti et al., 2014).

The advantages of a lightweight action camera in UAV photogrammetry has been highlighted by (Hastedt et al., 2016) using GoPro Hero4, with different acquisition modes. Their results suggested to apply the pre-corrected images together with pre-calibrated interior orientation parameters, which provided valid parameters and most reliable results. They have also recommended on the use of GoPro Studio for applying pre-correction of image, and Agisoft Lens for generating statistical information with chessboard pattern. Our methodological framework followed a similar approach as mentioned by (Hastedt et al., 2016 and Balletti et al., 2014). However, our results were less accurate, but in acceptable region compared to their results because their study area didn't include dense vegetation, where the automated feature detection and matching algorithm introduced some blunders (Remondino et al., 2011). Furthermore, it is highly recommended to have a sufficient overlap (~80-90%) between each consecutive images for feature matching and 3D reconstruction. Similarly, sufficient number of ground control points must be introduced and distributed throughout the project area, particularly around the periphery to ensure accurate and reliable calibration results for UAV photogrammetry. Likewise, the data from the modified action camera was free from Jello Effect (vibration, damping) due to the use of Image Stabilizing Gimbal especially designed for Mobius Action Camera (Quanum 3-axis brushless Gimbal) as demonstrated in Figure 3(a). Furthermore, the image acquisition was carried at an altitude of 200 m which covered large area, and supplied enough feature matches for SfM algorithm.

Various methods and protocols have been developed to test the feasibility of a modified camera system in agricultural health monitoring. For instance, (Hunt et al., 2010) studied the ability of digital color infrared camera modified through the replacement of NIR internal mirror filter with red light blocking filter in crop monitoring using UAV. The acquisition was carried out over two variably fertilized field of winter wheat in Queen Anne's County, Maryland, USA. Their results in terms of GNDVI was found to have a good correlation (R^2= 0.85) with LAI, which suggested that their approach was potential in providing accurate information on crop health. They collected imagery at 105 m and 210 m altitude, and applied tarpaulins of various color for the spectral and radiometric calibration of the modified camera. The application of a dual camera system for agricultural health monitoring was studied by (Wijitdechakul et al., 2016b), however their dual camera system decreased the spatial and radiometric accuracy while registering the images, due to the difference in grey level distribution between NIR and visible images (Hunt et al., 2010 and Rabatel et al., 2014). A study on the potential of digital camera to be applied as a multispectral sensor has been performed by (Lebourgeois et al., 2008) to monitor crop by examining a series of radiometric calibrations which reduced the distortions subjected to camera optics and environmental conditions. Their results suggested on addition of a preprocessing step for the raw images to correct the vignetting effect. Similarly, (Lelong et al., 2008) applied the combination of digital camera and spectral filters to design multispectral sensor for the application in precision farming. The images were computed for NDVI, which was compared with field measurement of LAI. Their results demonstrated a moderate correlation between NDVI results and LAI with R^2 of 0.82 and root square error of 0.57; concluding that their results from standard cameras is potential for precision agriculture; and further suggests researchers on simplifying and improving preprocessing step to establish more accurate results. Our calibration approach followed an approach similar to (Bourgeon et al., 2016) with direct measurements using spectroradiometer in the field under sunlight conditions to convert DN to reflectance measurements for the calculation of NDVI. Similar to their results, we observed the variation in light intensity with some saturation in the white calibration targets (DN >250). Furthermore, some targets had strong sensitivity to light source, effects of noise and environmental conditions. In order to optimize radiometric calibration, one must carefully select the number of required calibration targets by excluding targets with high saturation.

6. Conclusion

This study assessed the feasibility of an inexpensive modified infrared CMOS based action camera mounted on DJI Phantom 3 Professional in monitoring crop health. The action camera was modified by replacing the infrared filter with blue blocking filter, resulting in the camera configuration as R-G-NIR to compute NDVI; which was tested and validated against the field measurement of LAI. There was a moderate correlation between the NDVI results from the modified camera and the field estimates of LAI with an R^2 value of 0.843. Moreover, this camera setup has a great potential in precision agriculture; however, further research needs to focus on effective band separation by choosing a more suited band pass filters to achieve accurate results. This study is expected to assist farmers in agricultural decision making by constantly monitoring crop health using NDVI throughout the growth season. Finally, further research needs to focus on automation of SfM algorithm, reduction of the complexities in pre-processing, efficient geometric & radiometric calibration, and a simplified workflow to provide fast and accurate output to the end users.

Acknowledgment

This research was made possible through the financial support from Thammasat University: TU Basic and Applied Research Grant 2017. We would like to thank RS and GIS Department at Asian Institute of Technology, Thailand for their assistance in field validation, using LI-COR LAI 2000 Plant Canopy Analyzer.

References

Agarwal, S., Furukawa, Y., Snavely, N., Simon, I., Curless, B., Seitz, S. M. and Szeliski, R., 2011, Building Rome in a Day. *Communications of the ACM*. Vol. 54, No. 10, 105-112.

Alexandridis, T. K., Andrianopoulos, A., Galanis, G., Kalopesa, E., Dimitrakos, A., Katsogiannos, F. and Zalidis, G., 2017, An Integrated Approach to Promote Precision Farming as a Measure Toward Reduced-Input Agriculture in Northern Greece using a Spatial Decision Support System. Reference Module in Earth Systems and Environmental Sciences (Elsevier). 315–352.

Allahyari, M. S., Mohammadzadeh, M. and Nastis, S. A., 2016, Agricultural Experts' Attitude towards Precision Agriculture: Evidence from Guilan Agricultural Organization, Northern Iran. *Information Processing in Agriculture*, 3: 183-89.

Anupunt, P., 2002, Banana in Thailand, Advancing Banana and Plantain R &D in Asia and the Pacific. *Proceedings of the 10th INIBAP-ASPNET Regional Advisory Committee meeting held at Bangkok, Thailand*. Vol. 11: 149.

Atzberger, C., 2013, Advances in Remote Sensing of Agriculture: Context Description, Existing Operational Monitoring Systems and Major Information Needs. *Remote Sensing*, 5: 949-81.

Balletti, C., Guerra, F., Scocca, V. and Gottardi, C., 2015, 3D Integrated Methodologies for the Documentation and the Virtual Reconstruction of an Archaeological Site. *The International Archives of Photogrammetry, Remote Sensing and Spatial Information Sciences*, 40: 215.

Balletti, C., Guerra, F., Tsioukas, V. and Vernier, P., 2014, Calibration of Action Cameras for Photogrammetric Purposes. *Sensors*, 14: 17471-90.

Bendig, J., Yu, K., Aasen, H., Bolten, A., Bennertz, S., Broscheit, J., Gnyp, G. L. and Bareth, G., 2015, Combining UAV-Based Plant Height from Crop Surface Models, Visible, and near Infrared Vegetation Indices for Biomass Monitoring in Barley. *International Journal of Applied Earth Observation and Geoinformation*, 39: 79-87.

Bourgeon, M. A., Paoli, J. N., Jones, G., Villette, S. and Gée, C., 2016, Field Radiometric Calibration of a Multispectral on-the-go Sensor Dedicated to the Characterization of Vineyard Foliage. *Computers and Electronics in Agriculture*. 123: 184-94.

Bravo, C., Moshou, D., West, J., McCartney, A. and Ramon, H., 2003, Early Disease Detection in Wheat Fields using Spectral Reflectance., *Biosystems Engineering*, 84: 137-45.

D'Agostino, P., Antuono, G. and Pepe, F., 2015, Action Cameras in Digital Photogrammetry. Experiences of Comparison of Dense Point Clouds.

Distortion, GIMP Lens, 2013, Lens Distortion, Accessed July 22. https://docs.gimp.org/en/plug-in-lens-distortion.html.

Douterloigne, K., Gautama, S. and Philips, W., 2009, Fully Automatic and Robust UAV Camera Calibration using Chessboard Patterns. *In 2009 IEEE International Geoscience and Remote Sensing Symposium*, II-551-II-54.

Duane, C. B., 1971, Close-Range Camera Calibration. *Photogramm. Eng*, 37: 855-66.

Fan, L., Gao, Y., Brück, H. and Bernhofer, Ch., 2009a, Investigating the Relationship Between NDVI and LAI in Semi-Arid Grassland in Inner Mongolia using In-Situ Measurements. *Theoretical and Applied Climatology*, 95: 151-56.

Fan, L. Y., Gao, Y. Z., Brück, H. and Bernhofer, Ch., 2009b, Investigating the Relationship between NDVI and LAI in Semi-Arid Grassland in Inner Mongolia using In-Situ Measurements. *Theoretical and Applied Climatology*, 95: 151-56.

Ghazal, M., Khalil, Y. A. and Hajjdiab, H., 2015, UAV-Based Remote Sensing for Vegetation Cover Estimation using NDVI Imagery and Level Sets Method. *In 2015 IEEE International Symposium on Signal Processing and Information Technology* (ISSPIT), 332-37.

Gitelson, A. A., Kaufman, Y. J. and Merzlyak, M. N., 1996, Use of a Green Channel in Remote Sensing of Global Vegetation from EOS-MODIS. *Remote sensing of Environment*, 58: 289-98.

Hartley, R. and Zisserman, A., 2004, Multiple View Geometry in Computer Vision (Cambridge University Press: Cambridge).

Harwin, S., Lucieer, A. and Osborn, J., 2015, The Impact of the Calibration Method on the Accuracy of Point Clouds Derived using Unmanned Aerial Vehicle Multi-View Stereopsis. *Remote Sensing*, 7: 11933.

Hastedt, H., Ekkel, T. and Luhmann, T., 2016, Evaluation of the Quality of Action Cameras with Wide-Angle Lenses in UAV Photogrammetry. *International Archives of the Photogrammetry, Remote Sensing and Spatial Information Sciences*, 41.851-859.

Hedborg, J., Forssén, P. E., Felsberg, M. and Ringaby, E., 2012, Rolling Shutter Bundle Adjustment. *In 2012 IEEE Conference on Computer Vision and Pattern Recognition*. 1434-41.

Horning, N., 2013, Photo Monitoring Plugin, Accessed July 22. https://github.com/nedhorning/PhotoMonitoringPlugin/graphs/contributors.

Horning, N., 2015, Introducing the Calibration Plugin for ImageJ/Fiji', Accessed July 22. https://publiclab.org/notes/nedhorning/07-22-2015/introducing-the-calibration-plugin-for-imagej-fiji.

Hunt, E. R., Cavigelli, M., Daughtry, C. S. T., Mcmurtrey,J. E. and Walthall, C. L., 2005 Evaluation of Digital Photography from Model Aircraft for Remote Sensing of Crop Biomass and Nitrogen Status. *Precision agriculture*, 6: 359-78.

Hunt, E. R., Hively, W. D., Fujikawa, S. J., Linden, D. S., Daughtry, C. S. T. and McCarty, G. W., 2010, Acquisition of NIR-Green-Blue Digital Photographs from Unmanned Aircraft for Crop Monitoring. *Remote Sensing*, 2: 290-305.

Javernick, L., Brasington, J. and Caruso, B., 2014, Modeling the Topography of Shallow Braided Rivers using Structure-from-Motion Photogrammetry. *Geomorphology*, 213: 166-82.

Kelcey, J. and Lucieer, A., 2012, Sensor Correction of a 6-Band Multispectral Imaging Sensor for UAV Remote Sensing. *Remote Sensing*, 4: 1462-93.

Lamb, D. W. and Brown, R. B., 2001, PA—Precision Agriculture. *Journal of Agricultural Engineering Research.* 78: 117-25.

Lebourgeois, V., Bégué, A., Labbé, S., Mallavan, B., Prévot,L. and Roux, B., 2008, Can Commercial Digital Cameras be used as Multispectral Sensors? A Crop Monitoring Test. *Sensors*, 8(11), 7300-7322.

Lelong, C. C. D., Burger, P., Jubelin, G., Roux, B., Labbé, S. and Baret, F., 2008, Assessment of Unmanned Aerial Vehicles Imagery for Quantitative Monitoring of Wheat Crop in Small Plots. *Sensors*, 8: 3557-85.

LLC, 2017, Agisoft Photoscan User Manual: Professional Edition', Agisoft LLC, Accessed June 22. http://www.agisoft.com/pdf/photoscan-pro_1_3_en.pdf.

Lowe, D. G., 2004, Distinctive Image Features from Scale-Invariant Keypoints. *International Journal of Computer Vision*, 60: 91-110.

Marti, J., Bort, J. Slafer, G. A. and Araus, J. L., 2007, Can Wheat Yield be Assessed by Early Measurements of Normalized Difference Vegetation Index?', *Annals of Applied Biology*. 150: 253-57.

Meng, J., Du, X. and Wu, B., 2013, Generation of High Spatial and Temporal Resolution NDVI and its Application in Crop Biomass Estimation. *International Journal of Digital Earth*, 6: 203-18.

Mobambo, K. N., Gauhl, F., Vuylsteke, D., Ortiz, R., Pasberg-Gauhl, C. and Swennen, R., 1993, Yield Loss in Plantain from Black Sigatoka Leaf Spot and Field Performance of Resistant Hybrids. *Field Crops Research*, 35: 35-42.

Nijland, W., Jong, R. D., De Jong, S. M., Wulder, M. A., Bater, C. W. and Coops, N. C., 2014, Monitoring Plant Condition and Phenology using Infrared Sensitive Consumer Grade Digital Cameras. *Agricultural and Forest Meteorology*, 184: 98-106.

Rabatel, G., Gorretta, N. and Labbe, S., 2014, Getting Simultaneous Red and Near-Infrared Band Data from a Single Digital Camera for Plant Monitoring Applications: Theoretical and Practical Study. *Biosystems Engineering*, 117: 2-14.

Remondino, F., Barazzetti, L., Nex, F., Scaioni, M. and Sarazzi, D., 2011, UAV Photogrammetry for Mapping and 3d Modeling–Current Status and Future Perspectives. *International Archives of the Photogrammetry, Remote Sensing and Spatial Information Sciences*, 38: C22.

Scharstein, D. and Szeliski. R., 2002, A Taxonomy and Evaluation of Dense Two-Frame Stereo Correspondence Algorithms. *International Journal of Computer Vision*, 47: 7-42.

Schindelin, J., Arganda-Carreras, I., Frise, E., Kaynig, V., Longair, M., Pietzsch, T., Preibisch, S., Rueden, C., Saalfeld, S. and Schmid, B., 2012, Fiji: an Open-Source Platform for Biological-Image Analysis. *Nature Methods*, 9: 676-82.

Shaw, R., Lark, R. M., Williams, A. P., Chadwick, D. R. and Jones, D. L., 2016, Characterising the within-Field Scale Spatial Variation of Nitrogen in a Grassland Soil to Inform the Efficient Design of In-Situ Nitrogen Sensor Networks for Precision Agriculture. *Agriculture, Ecosystems and Environment*, 230: 294-306.

Sona, G., Pinto, L., Pagliari, D., Passoni, D. and Gini, R., 2014, Experimental Analysis of Different Software Packages for Orientation and Digital Surface Modelling from UAV Images. *Earth Science Informatics*, 7: 97-107.

Tucker, C. J, Slayback, D. A., Pinzon, J. E., Los, S. O., Myneni, R. B. and Taylor, M. G., 2001, Higher Northern Latitude Normalized Difference Vegetation Index and Growing Season Trends from 1982 to 1999, *International Journal of Biometeorology*, 45: 184-90.

Turner, D., Lucieer, A. and Watson, C., 2012, An Automated Technique for Generating Georectified Mosaics from Ultra-High Resolution Unmanned Aerial Vehicle (UAV) Imagery, Based on Structure from Motion (SfM) Point Clouds. *Remote Sensing*, 4: 1392.

Turner, D. W., Jeanie, A. F. and Thomas, D. S., 2007, Environmental Physiology of the Bananas (Musa spp.). *Brazilian Journal of Plant Physiology*, 19: 463-84.

Ullman, S., 1979, The Interpretation of Structure from Motion. *Proceedings of the Royal Society of London B: Biological Sciences*, 203: 405-26.

Velasquez, L. C., Argueta, J. and Mazariegos, K., 2016, Implementation of a Low Cost Aerial Vehicle for Crop Analysis in Emerging Countries. *In 2016 IEEE Global Humanitarian Technology Conference* (GHTC), 21-27.

Verhoeven, G., Doneus, M., Briese, Ch. and Vermeulen, F., 2012, Mapping by Matching: a Computer Vision-Based Approach to Fast and Accurate Georeferencing of Archaeological Aerial Photographs. *Journal of Archaeological Science*, 39: 2060-2070.

Verhoeven, G., 2011, Taking Computer Vision Aloft – Archaeological Three-Dimensional Reconstructions from Aerial Photographs with Photoscan. *Archaeological Prospection*, 18: 67-73.

Wijitdechakul, J., Sasaki, S., Kiyoki, Y. and Koopipat, C., 2016a, UAV-Based Multispectral Image Analysis System with Semantic Computing for Agricultural Health Conditions Monitoring and Real-Time Management. *In 2016 International Electronics Symposium (IES)*, 459-64.

Wijitdechakul, J., Sasaki, S., Kiyoki,Y. and Koopipat, C., 2016b, UAV-Based Multispectral Image Analysis System with Semantic Computing for Agricultural Health Conditions Monitoring and Real-Time Management. *In Electronics Symposium (IES), 2016 International*, 459-64.

Wu, C., 2013, Towards Linear-Time Incremental Structure from Motion. In 3DTV-Conference, 2013 International Conference on, *IEEE*, 127-34.

Zhang, C. and Kovacs, J. M., 2012, The Application of Small Unmanned Aerial Systems for Precision Agriculture: A Review. *Precision Agriculture*, 13: 693-712.

Zigadlo, J. P., Holden, C. L., Schrader, M. E. and Vogel, R. M., 2001, Electronic Color Infrared Camera. In. Google Patents.